Interference Management by Vertical Beam Control Combined with Coordinated Pilot Assignment and Power Allocation in 3D Massive MIMO Systems

Guomei Zhang[1], Bing Wang[1], Guobing Li[1], Fei Xiang[2] and Gangming lv[1]
[1] Department of Information and Communication Engineering, Xi'an Jiaotong University
Xi'an, 710049, P. R. China
[e-mail: zhanggm@mail.xjtu.edu.cn, wang.bing123@stu.xjtu.edu.cn]
[e-mail: gbli@mail.xjtu.edu.cn, gmlv@mail.xjtu.edu.cn]
[2] Department of Baseband Algorithm, R&D center of ZTE corporation
Xi'an, 710065, P. R. China
[e-mail: xiang.fei1@zte.com.cn]
*Corresponding author: Guomei Zhang

Received January 12, 2015; revised May 20, 2015; accepted June 21, 2015; published August 31, 2015

Abstract

In order to accommodate huge number of antennas in a limited antenna size, a large scale antenna array is expected to have a three dimensional (3D) array structure. By using the Active Antenna Systems (AAS), the weights of the antenna elements arranged vertically could be configured adaptively. Then, a degree of freedom (DOF) in the vertical plane is provided for system design. So the three-dimension MIMO (3D MIMO) could be realized to solve the actual implementation problem of the massive MIMO. However, in 3D massive MIMO systems, the pilot contamination problem studied in 2D massive MIMO systems and the inter-cell interference as well as inter-vertical sector interference in 3D MIMO systems with vertical sectorization exist simultaneously, when the number of antenna is not large enough. This paper investigates the interference management towards the above challenges in 3D massive MIMO systems. Here, vertical sectorization based on vertical beamforming is included in the concerned systems. Firstly, a cooperative joint vertical beams adjustment and pilot assignment scheme is developed to improve the channel estimation precision of the uplink with pilots being reused across the vertical

This work is supported by National Natural Science Foundation of China (NSFC) under grant 61401350, the National 863 Program of China under Grant 2014AA01A707 and the Research Fund of ZTE Corporation.

http://dx.doi.org/10.3837/tiis.2015.08.003 **ISSN : 1976-7277**

sectors. Secondly, a downlink interference coordination scheme by jointly controlling weight vectors and power of vertical beams is proposed, where the estimated channel state information is used in the optimization modelling, and the performance loss induced by pilot contamination could be compensated in some degree. Simulation results show that the proposed joint optimization algorithm with controllable vertical beams' weight vectors outperforms the method combining downtilts adjustment and power allocation.

Keywords: Massive MIMO, 3D MIMO, vertical beams, power allocation, pilot contamination

1. Introduction

WITH the explosive growth of wireless data service, one of the important design considerations in next generation cellular networks is to improve the spectral efficiency as far as possible. Several approaches have been introduced to meet this demand, such as cognitive radio (CR) technology [1,2] and massive MIMO [3]. CR has been proved to be one of the most promising candidate solutions to solve the problem of scarce spectrum resources [4]. On the other hand, massive MIMO where base stations are equipped with large-scale antennas could improve the system spectral efficiency effectively [3] and has received wide investigation recently. Channel state information (CSI) is usually obtained on the basis of pilot sequences transmitted by users in massive MIMO TDD system. Unfortunately, the length of pilot sequences is limited by the coherence time, so the same set of orthogonal pilot sequences needs to be re-used among cells. As a result, the channel estimation by non-orthogonal pilots in neighboring cells contaminates each other, which is called pilot contamination [5]. In massive MIMO systems, previous research has shown that, when the number of base station antennas tends to infinity, system performance is limited only by pilot contamination [3]. Many schemes have been implemented to reduce pilot contamination, including effective channel estimation algorithms [6,7], robust precoding algorithms [8] and pilot pattern design [9]. Authors of [6], [7] have proposed an eigenvalue decomposition-based channel estimation approach and a Bayesian estimator to mitigate pilot contamination by improving channel estimation precision. A multi-cell MMSE based precoding method with coordination among base stations is studied to overcome pilot contamination problem in [8]. Both intra-cell interference and inter-cell interference caused by pilot contamination could be reduced by this precoder. A time-shifted pilot transmission scheme, where the pilots of the cells in one group are transmitted simultaneously with the downlink data in other cell groups, is presented in [9], where the interference among cell groups vanishes with infinite number of antennas. The analysis shows that all the interference coming from cells in different groups vanishes with infinite number of antennas and the pilot contamination is suppressed. However, all the methods mentioned above have just considered the antenna propagation in horizontal domain.

In reality, considering the huge number of antennas and the limited antenna size, the massive MIMO array is expected to be implemented in a uniform planar array (UPA) structure. By applying AAS, the weight coefficients of the antennas arranged vertically could be adaptively configured and the DOF of vertical dimension is provided. Therefore, 3D MIMO is introduced [10]. Then, an ideal of exploring the vertical DOF to reduce pilot contamination further occurs to us.

A typical 3D MIMO technology is cell splitting in both the horizontal and the vertical plane. The vertical cell splitting (or sectorizing) based on vertical beamforming is a typical technology to explore the vertical DOF and an improvement of the cell spectral efficiency can be reached by including the vertical sectoring [11]. Although, the work of [3] has proved that all the impacts of uncorrelated inter-cell interference and noise disappear as the number of antennas grows without limit, this is not the case for the practical 3D MIMO system with tens to hundreds of antennas rather than infinite antennas at base station. Meanwhile, the introduction of vertical sectorization would bring stronger interference, including not only inter-cell interference but also inter-vertical sector interference. In order to control the various interferences, many schemes have been proposed. In [12], an optimization method to find the optimum downtilts and powers of the two vertical sectors' beams based on the particle swarm optimization (PSO) algorithm is proposed. In [13], a joint optimization problem to coordinate interference in 3D-MIMO OFDMA networks is established, where resource block allocation, power controlling and downtilt adjustment are jointly optimized. The above two schemes both expect to improve the system sum-rate by adjusting the downtilt rather than the weight vector of antenna array. The weight vector optimization of antenna array is considered in [17] and [18]. In [17], the weight vector of 3D beam pattern is designed to minimize transmit power and a sectorizing strategy is proposed for massive MIMO system. An optimized beamforming design for vertical sectorization to suppress inter-vertical sector interference is proposed in [18]. However, the optimization objects of [17] and [18] are not to improve the spectral efficiency directly, which is the more popular performance metric of the system. Moreover, all of the above works have assumed perfect CSI without considering the pilot contamination problem, which would occur when base stations equipped with massive antennas serve a large number of users simultaneously. Especially, when the number of users served by each vertical sector is large and the pilot sequences have to be reused among sectors, the pilot contamination would become more serious

Unlike previous works, the aim of this paper is to improve the system spectral efficiency, through designing the weight vectors of vertical beams to effectively manage various interferences in the vertical sectorizing massive MIMO system. Firstly, in order to meet the challenge of pilot contamination caused by vertical sectorization, an iterative weight vectors adjustment and pilot scheduling process is applied in uplink. Secondly, joint weight vectors adjustment and power allocation for vertical beams are performed in downlink to coordinate the inter-cell interference and the inter-verical sector interference. The difference of our downlink scheme from the methods in [12] and [13] is that the vertical beam can be controlled more precisely by adjusting the weight vector of antenna array

based on an applicable downtilt angle rather than only adjusting the downtilt. On the other hand, the downlink optimization problem is built on the estimated channel information of uplink, so the impact of pilot contamination is included. Therefore, the solution of our optimization problem could suppress the impact of pilot contamination indirectly.

2. System Description

2.1 System Model

We consider a coordination cluster of $L \geq 2$ horizontal sectors. Taking advantage of two vertical beams, every horizontal sector is divided into two vertical sectors. Each sector is served by a UPA with *M* antennas, where the number of horizontal antennas and vertical antennas is N_t and N_v respectively. $K(K << M)$ single-antenna users are uniformly and randomly distributed in each horizontal sector. Then, a cooperation cluster is shown by the dashed line box in Fig.1, where $\theta_{D,l0}$ and $\theta_{D,l1}$ indicate the near vertical sector and far vertical sector specific downtilt of the *l*-th horizontal sector in the coordination cluster, respectively. In the case of no confusion, a horizontal sector is referred as a cell below, which is served by a base station.

A channel model including correlations among the antennas is considered. The channel vector from the k-th user of the *l*-th cell to the UPA of the *j*-th cell is expressed as $\mathbf{b}_{jlk} = \sqrt{\beta_{jlk}}\mathbf{h}_{jlk} = \sqrt{\beta_{jlk}}\mathbf{R}_{jlk}^{\frac{1}{2}}\boldsymbol{\omega}_{jlk}$ [7,20] and $\mathbf{b}_{jlk} \in C^{M\times 1}$. Here β_{jlk} represents the large-scale fading coefficient including geometric attenuation and shadow fading, which is assumed to be constant with respect to the antenna index of the UPA and known by all the base stations in the cooperation cluster. $\mathbf{R}_{jlk} = E\left\{\mathbf{h}_{jlk}\mathbf{h}_{jlk}^H\right\}$ is the fast fading channel covariance matrix. In Section 5, the calculation of $\mathbf{R}_{jlk}$ would be given for the simplified 3D spatial channel model based on finite-scattering physical modelling. The elements of the vector $\boldsymbol{\omega}_{jlk}$ are assumed to be independent and identically distributed (i.i.d.) circularly symmetric complex Gaussian random variables with zero-mean and one-variance. We further assume a time block flat-fading channel. The fast fading coefficients stay the same during a coherence interval of T symbols and change independently for different coherence blocks.

UPA is comprised of several elements which are controlled by different antenna ports. Since the target of this work is to investigate how to explore the vertical DOF, the two-dimensional propagation in the vertical plane is concerned. So the omni-directional antenna pattern in the horizontal dimension is assumed in system design. That is to say the beam gain is independent with the azimuthal angle. Then, according to the structure of UPA, the vertical beam pattern of the near sector in the *l*-th cell could be expressed as [17]

$$A(\theta_{D,l0},\theta) = \mathbf{w}_{l0}^H\mathbf{B}_r(\theta,\theta_{D,l0}), \quad (1)$$

where $\mathbf{w}_{l0} \in C^{M\times 1}$ denotes the weight vector of antennas for the near sector. Same as the work [14], the influence of antenna weights on the transmission is included into the beam pattern by Eq. (1). θ is the elevation angle in spherical coordinates and $\theta_{D,l0}$ is the downtilt angle of the vertical beam in near sector. In Eq.(1), $\mathbf{w}_{l0} \in C^{M\times 1}$ denotes the weight vector of antennas for the near sector. Moreover, $\mathbf{B}_r(\theta,\theta_{D,l0}) \in C^{M\times 1}$ is the active element response vector, and its $((n-1)N_v+m)$-th element is the gain of the *m*-th row and *n*-th column antenna element of the antenna array, which could be denoted as

$$B_{r,m,n}(\theta,\theta_D) = G_v(\theta,\theta_D)e^{j\frac{2\pi}{\lambda}nd_z\cos(\theta-\theta_D)+j\frac{2\pi}{\lambda}md_y\sin(\theta-\theta_D)}, \quad (2)$$

where d_y and d_z are the distances between the two adjacent horizontal and vertical antenna elements, respectively. And $G_v(\theta,\theta_D) = -\min\{12[(\theta-\theta_D)/\theta_{3dB}]^2, 20\}$ dB is the vertical pattern gain of single antenna, where θ_{3dB} is the vertical HPBW (Half Power Beam Width) angle. From (1), it can be seen that the vertical beam pattern is dependent on both the downtilt and the antenna weight vector. In this case, the composite channel between the k_0-th user in the near sector of the *l*-th cell and the *l*-th BS is given by

$$\mathbf{c}_{llk_0} = \mathbf{b}_{llk_0}\sqrt{A(\theta_{D,l0},\theta_{llk_0})}. \quad (3)$$

In our system, K' users distributed in the same vertical sector would be served simultaneously by one vertical beam on the same time-frequency resource.

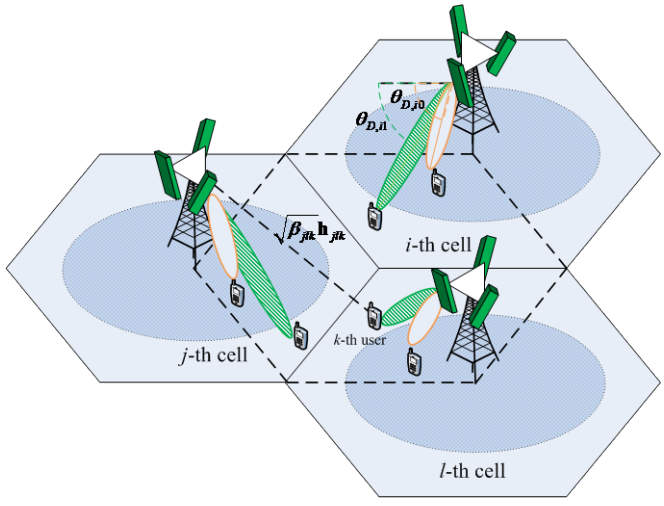

Fig. 1. System model

Moreover, TDD transmission protocol is considered here. According to channel reciprocity in TDD systems, the channel gains are the same for the forward and reverse

links. Only two phases in each channel coherence interval are focused on. First, each user sends a pilot sequence to its BS and the BS uses this pilot to estimate the corresponding channel vector. Then, the BS transmits downlink data to its users by using the channel estimates of uplink to form the precoder.

2.2 Uplink Channel Estimation

In the uplink training phase of the massive MIMO system, it is normally assumed that mutually orthogonal pilots are allocated to the users within the same cell and the same set of orthogonal pilots is reused among cells [3]. Therefore, the number of users served by a base station simultaneously is limited by the length of pilot sequence. Under the case of vertical sectorization, the same set of orthogonal pilots could be reused among the vertical sectors. As a result, the length of pilot sequence could decrease while the total number of users in a cell does not change. Or, the more users could be served in a cell while the length of pilot sequence remains the same.

During the channel estimation period, the downtilt of each UPA is fixedly selected as the average elevations of the users in the corresponding vertical sector. Assuming that the number of the users in each near sector and far sector is K_0 and K_1, respectively. Meanwhile, $K_0+K_1=K$. The length of a pilot sequence must meet $\tau \geq \max(K_0, K_1)$. Furthermore, we define a intra-cell pilot reuse factor as the ratio of the pilot length to the number of users in a cell, i.e $r = \tau / K$. For the worst case that the pilot contamination degree is the highest, there are $K_0=K_1=K' = K/2$ and $r = 0.5$. In this case, the users indexed by k_0 in the near sector and k_1 in the far sector are assumed to send the same pilot sequence $\mathbf{\Psi}_k$ (a $1\times\tau$ vector). For the near sector of the *j*-th cell, the signal received at the BS is

$$\mathbf{y}_j = \sqrt{p_r}\sum_{l=1}^{L}\sum_{k=1}^{K'}(\mathbf{b}_{jlk_0}\sqrt{A(\theta_{D,j0},\theta_{jlk_0})_u} + \mathbf{b}_{jlk_1}\sqrt{A(\theta_{D,j0},\theta_{jlk_1})_u})\mathbf{\Psi}_k + \mathbf{z}_j, \tag{4}$$

where p_r denotes the average power (during pilot transmission) of each user. $A(\cdot)_u$ is the vertical beam pattern of the BS antennas for uplink and is defined as (1). $\theta_{D,j0}$ is the downtilt angle of the UPA for the near sector in the *j*-th cell. $\theta_{D,jlk_i}(i=0,1)$ is the elevation angle from the k_i-th user of the *l*-th cell to the *j*-th BS. Here, θ_{D,jlk_i} is taken as the average angle of all the paths' vertical AOA (angle of arrival) in the multipath spatial channel between the user and the BS. It is used to represent the average effect of multiple paths. $\mathbf{z}_j$ is the additive noise vector of the receiving antenna array, the elements of which are i.i.d $CN(0,1)$ random variables.

By least square (LS) estimation, the estimate of the composite channel vector for the user $k_i(i=0,1)$ in the *j*-th cell is $\hat{\mathbf{c}}_{jjk_i}^{LS} = \dfrac{\mathbf{y}_j\mathbf{\Psi}_k^H}{\tau\sqrt{p_r}}$. This process is same as the channel

estimation in 2D massive MIMO. While, considering the design targets of uplink and downlink being different, their antenna weights should be variant. Furthermore, their vertical beam patterns are different, even for the same downtilt and elevation angle. So we need to estimate the common $\mathbf{b}_{jjk_i}$ rather than $\mathbf{c}_{jjk_i}^{LS}$ in uplink. It could be obtained that

$$\hat{\mathbf{b}}_{jjk_i}^{LS}=\frac{\hat{\mathbf{c}}_{jjk_i}^{LS}}{\sqrt{A(\theta_{D,ji},\theta_{jjk_i})_u}}=\mathbf{b}_{jjk_i}+\mathbf{b}_{jjk_{\bar{T}}}\frac{\sqrt{A(\theta_{D,ji},\theta_{jjk_{\bar{T}}})_u}}{\sqrt{A(\theta_{D,ji},\theta_{jjk_i})_u}}+\sum_{l=1,l\neq j}^{L}\sum_{n=0}^{1}\mathbf{b}_{jlk_n}\frac{\sqrt{A(\theta_{D,ji},\theta_{jlk_n})_u}}{\sqrt{A(\theta_{D,ji},\theta_{jjk_i})_u}}+\frac{\mathbf{z}_j\mathbf{\Psi}_k^H}{\tau\sqrt{p_r A(\theta_{D,ji},\theta_{jjk_i})_u}}. \tag{5}$$

Moreover, we can derive that the normalized estimation mean squared error (MSE) with $M\to\infty$ is

$$E_{jk_i}^{mse}=\lim_{M\to\infty}E\left\{\frac{\left\|\hat{\mathbf{b}}_{jjk_i}^{LS}-\mathbf{b}_{jjk_i}\right\|_F^2}{\left\|\mathbf{b}_{jjk_i}\right\|_F^2}\right\}=\frac{A(\theta_{D,ji},\theta_{jjk_{\bar{T}}})_u}{A(\theta_{D,ji},\theta_{jjk_i})_u}\frac{\beta_{jjk_{\bar{T}}}}{\beta_{jjk_i}}+\sum_{l=1,l\neq j}^{L}\sum_{n=0}^{1}\frac{A(\theta_{D,ji},\theta_{jlk_n})_u}{A(\theta_{D,ji},\theta_{jjk_i})_u}\frac{\beta_{jlk_n}}{\beta_{jjk_i}}. \tag{6}$$

It can be seen from (6) that the asymptotic MSE of the LS estimators in 3D massive MIMO depends on both the large scale fading coefficients and the beam gains due to the vertical beamforming. This is just the difference from the 2D massive MIMO. The accuracy of channel estimation may be improved if these parameters could be taken advantage of or be adjusted.

2.3 Downlink Transmission

In the downlink data transmission phase, we still consider the case of $r=0.5$ and two vertical beams in each cell. Without loss of generality, the i_0-th user in the near sector of the *j*-th cell is the target user and its signal is q_{ji_0}. We assume that q_{ji} are i.i.d, $E\{q_{ji}\}=0$ and $E\{q_{ji}^H q_{ji}\}=1$. If the conjugate precoding scheme, which is widely adopted in massive MIMO, is used for user data, then the precoding vector of the user k_0 in the *j*-th cell is $\mathbf{a}_{jjk_0}=\frac{\hat{\mathbf{b}}_{jjk_0}^*\sqrt{A(\theta_{D,j0},\theta_{jjk_0})_d}}{\left\|\hat{\mathbf{b}}_{jjk_0}^*\sqrt{A(\theta_{D,j0},\theta_{jjk_0})_d}\right\|}=\frac{\hat{\mathbf{b}}_{jjk_0}^*}{a_{jjk_0}\sqrt{M}}$, where $a_{jjk_0}=\left\|\hat{\mathbf{b}}_{jjk_0}^*\right\|/\sqrt{M}$. The interference is caused by the transmission of all base stations in a cluster, then the noisy signal received by the i_0-th near sector user in the *j*-th cell is

$$x_{ji_0}=\sum_{l=1}^{L}\left(\sum_{k_0=1}^{K'}\sqrt{P_{l0}}\mathbf{b}_{lji_0}^T\sqrt{A(\theta_{D,l0},\theta_{lji_0})_d}\mathbf{a}_{llk_0}q_{lk_0}+\sum_{k_1=1}^{K'}\sqrt{P_{l1}}\mathbf{b}_{lji_0}^T\sqrt{A(\theta_{D,l1},\theta_{lji_0})_d}\mathbf{a}_{llk_1}q_{lk_1}\right)+z_{ji_0}, \tag{7}$$

where $A(\cdot)_d$ is the vertical beam pattern of the BS antenna for downlink. The powers of the beams serving the near and far sector of *l*-th cell are P_{l0} and P_{l1}, respectively. $P_{l0}+P_{l1}=P$. z_{ji_0} is the additive white Gaussian noise and $z_{ji_0}\in CN(0,1)$.

Denote $\mathbf{g}_{ji_0}^{lk}=\sqrt{P_{lk}}\mathbf{b}_{lji_0}^T\sqrt{A(\theta_{D,lk},\theta_{lji_0})_d}\,(k=0,1)$, then (7) could be rewritten as

$$x_{ji_0}=\mathbf{g}_{ji_0}^{j0}\mathbf{a}_{jji_0}q_{ji_0}+\sum_{k_0=1,k_0\neq i_0}^{K'}\mathbf{g}_{ji_0}^{j0}\mathbf{a}_{jjk_0}q_{jk_0}+\sum_{k_1=1}^{K'}\mathbf{g}_{ji_0}^{j1}\mathbf{a}_{jjk_1}q_{jk_1}+\sum_{l=1,l\neq j}^{L}\sum_{k_n=1}^{K'}\sum_{n=0}^{1}\mathbf{g}_{ji_0}^{l\mathrm{n}}\mathbf{a}_{llk_n}+z_{ji_0}. \quad (8)$$

In (8), the first term is the desired signal, and all other terms form the effective noise, namely intra-sector interference, inter-sector interference, inter-cell interference and thermal noise. Further, we could obtain the SINR and achievable rate of the i_0-th user in the near sector of the *j*-th cell, which are given by

$$\gamma_{ji_0}=\frac{\left|\mathbf{g}_{ji_0}^{j0}\mathbf{a}_{jji_0}\right|^2}{\sum_{k_0=1,k_0\neq i_0}^{K'}\left|\mathbf{g}_{ji_0}^{j0}\mathbf{a}_{jjk_0}\right|^2+\sum_{k_1=1}^{K'}\left|\mathbf{g}_{ji_0}^{j1}\mathbf{a}_{jjk_1}\right|^2+\sum_{l=1,l\neq j}^{L}\left(\sum_{k_0=1}^{K'}\left|\mathbf{g}_{ji_0}^{l0}\mathbf{a}_{llk_0}\right|^2+\sum_{k_1=1}^{K'}\left|\mathbf{g}_{ji_0}^{l1}\mathbf{a}_{llk_1}\right|^2\right)+1} \quad (9)$$

and

$$R_{ji_0}=\frac{T-\tau}{T}\log_2(1+\gamma_{ji_0}). \quad (10)$$

In (10), the coefficient $(T-\tau)/T$ is the result of taking the pilot overhead into account. From Eq. (9), we can see that the adjustment of antennas' weight vector, which decides the vertical beam pattern, will affect the SINR of users since the transmitted data undergoes the composite channel. Therefore, in 3D massive MIMO, the adjustment of antennas weight vector could be also included for better system performance, in addition to the design of the user data precoding vector. This is just a major job of Section 4.

2.4 Pilot Contamination

From (5), we can see that pilot contamination becomes more serious after applying vertical sectorization and reusing pilot sequences among vertical sectors. Moreover, the stronger interference to the users within the same sector or in the other sectors would be created. Based on the asymptotic of random matrix theory, we can obtain the asymptotic SINR expressed as (11). And the detail derivation of approximate SINR will be presented in Appendix.

$$\lim_{M\to\infty}\gamma_{ji_0}=\frac{P_{j0}\beta_{jji_0}^2/a_{jji_0}^2A(\theta_{D,j0},\theta_{jji_0})_d}{P_{j1}\frac{\beta_{jji_0}^2}{a_{jji_1}^2}A(\theta_{D,j1},\theta_{jji_0})_d\frac{A(\theta_{D,j1},\theta_{jji_0})_u}{A(\theta_{D,j1},\theta_{jji_1})_u}+\sum_{\substack{l=1\\l\neq j}}^{L}\beta_{ljj_0}^2[\sum_{n=0}^{1}P_{l\mathrm{n}}A(\theta_{D,l\mathrm{n}},\theta_{ljj_0})_d\frac{A(\theta_{D,l\mathrm{n}},\theta_{ljj_0})_u}{a_{llj_n}^2A(\theta_{D,l\mathrm{n}},\theta_{llj_n})_u}]} \quad (11)$$

As we can see from (11), in 3D massive MIMO system, the interference still comes from the users sharing the same pilot sequence, which is the same as the traditional massive MIMO. The difference is the asymptotic SINR not only depends on the large-scale fading coefficients but also the antenna gains. Another issue to be discussed is the impact of the large *M* on the beam pattern. We find that, when the number of antennas increases, the main lobe beamwidth decreases, meanwhile, the number of sidelobes and pattern nulls increases. Furthermore, there are more weights of antennas we can design to control the vertical beams more precisely and coordinate various interferences more effectively.

3. Coordinated Joint Vertical Beams Adjustment and Pilot Assignment in Uplink

We have seen from (5) that the accuracy of channel estimation declined seriously, because pilot sequences are reused among sectors and the number of interference items increased nearly two times. Since the strength of pilot contamination is related to the large-scale fading coefficients of the interference links created by the users who adopt the same pilot sequence, a coordinated pilot assignment strategy basing on the large scale fading information had been proposed to improve the accuracy of channel estimation in massive MIMO [4]. Its basic idea is to let the users with weak mutual interference use the same pilot.

On the other hand, it can still be seen from (5) that the strength of pilot contamination also depends on the vertical beam pattern of uplink. If the vertical beams of every sector could be controlled jointly with the pilot assignment, the performance of channel estimation may be improved further. Therefore, we would investigate a joint pilot assignment and weight vectors adjustment of vertical beams for the uplink in 3D massive MIMO system.

In the 3D massive MIMO system of **Fig. 1,** for the case of $r = 0.5$, one pilot sequence would be assigned to $2L$ users simultaneously, each of which comes from one of the 2L sectors. Let U_k denote the set of selected users who transmit pilot sequence $\boldsymbol{\psi}_k$ and S_k denote the corresponding vertical sector set. The user set of the *i*-th sector is denoted by Ξ_i with the size of $K' = K/2$. For a given user set U_k, the utility function of pilot scheduling can be expressed as

$$F(U_k) = \sum_{j=1}^{|U_k|} E_j^{mse}(U_k), \tag{12}$$

where $|U_k|$ is the size of user set U_k and $|U_k| = 2L$. $E_j^{mse}(U_k)$ is the asymptotic MSE of LS estimation for the *j*-th user in the set U_k, who locates in the *j*-th vertical sector of S_k, and it has an expression of Eq.(6).

Then, the iterative pilot scheduling and weight vectors adjusting of vertical beams perform in the following procedure.

Step 1: Pilot Scheduling Scheme.

In this step, the weight vector of each vertical beam is fixed for each sector. Similar to [7], the principle of the pilot scheduling is to minimize the utility function defined in (12) and the classical greedy search approach is used. The detail is given in the follows.

1) Initialize $U_1 = \varnothing, \ldots, U_{K'} = \varnothing$ and $\Xi_1, \ldots, \Xi_{2L} = \{1, \ldots, K'\}$.

2) For $k = 1, \ldots, K'$ do:

Select a user $j_{1,k}$ randomly from the user set of the first sector and $j_{1,k} \in \Xi_1$. Assign the pilot sequence $\boldsymbol{\Psi}_k$ to user $j_{1,k}$ and let $\Xi_1 = \Xi_1 / j_{1,k}$ (i.e., remove the user $j_{1,k}$ from the user set of Ξ_1).

For $l = 2,3,\ldots,2L$ do:

$$j_{l,k} = \arg\min_{j \in \Xi_l} F\left\{U_k \cup \{j\}\right\}, U_k \leftarrow U_k \cup \left\{j_{l,k}\right\}, \Xi_l = \Xi_l / j_{l,k} .$$

End

Note: The inner loop is to select user one by one from the rest 2L-1 vertical sectors. And the criteria of choosing a new user is that the utility function of Eq.(12) could be minimized if it is added to the selected user set. Finally, these selected users would use the same pilot sequence of $\mathbf{\Psi}_k$.

End

Note: The outer loop is to iterate the indices of all pilot sequences and determines the user set for each pilot one by one. And the greedy search of a user set U_k *is executed independently for each k.*

Step 2: Weight Vectors Adjustment of Vertical Beams.

After the way of pilot assignment for the users is determined, the weight vectors of vertical beams would be optimized to minimize the total level of the channel estimation MSE. The optimization objective is expressed as,

$$\min_{\{\mathbf{w}_{ji}, i \in \{0,1\}\}} \sum_{k=1}^{K'} \sum_{j=1}^{|U_k|} E_j^{mse}(U_k) \tag{13}$$

Considering the complexity and difficulty of the above optimization problem, particle swarm optimization (PSO) optimization algorithm is applied. The details of resolving problem (13) based on PSO algorithm are similar to the problem (14) in Section 4, which can be referred to Part 2 in Section 4.

The processions of the pilot scheduling and weight vectors adjustment are executed iteratively until the total asymptotic MSE of channel estimation could not reduce further. In order to ensure the convergence of the iterative process, we should make sure that the channel estimation MSE in Step 1 of current iteration is less than that of the last iteration. Otherwise, the iteration is over.

The above optimization process is only based on the slowly varying information including the elevation of users and large-scale fading coefficient. For example, in the snapshot based simulation, we would execute the above process once for each drop, rather than for each coherence interval. Therefore, the proposed uplink scheme induces a small increase of system complexity.

4. Joint Weight Vectors Adjustment and Power Allocation

From (11), we can see that the interference in 3D massive MIMO system is related to the beam pattern and transmit power of each vertical sector. Therefore, if the beam pattern and power of each vertical sector in a cluster could be controlled reasonably, the various interferences would be coordinated effectively. In addition to the inter-sector interference and inter-cell interference, the negative impact on system performance caused by the

precoding matrices, which are jammed by pilot contamination, would be also reduced to some extent.

To control the beam pattern, we can not only adjust the downtilt of a UPA, but also design the weight vector of a UPA. In the existing literatures [12] and [13], they control the beam pattern by adjusting the downtilt. Our scheme is different from theirs'. For each vertical sector, we firstly select a reasonable downtilt according to the position distribution of users, then adjust the weight vector of antennas dynamically. Thus the vertical beam pattern could be controlled more precisely and flexibility.

In downlink transmission, the objective of our scheme is to maximize the spectral efficiency of a coordination cluster, subject to per cell power, near sector and far sector specific weight vector constraints. We determine an appropriate critical downtilt of each cell based on the elevation angles of users and divide the users into two sectors. Let the near sector has the same number of users as the far sector. Then calculate the near and far sector users' average elevation angle $\bar{\theta}_{l0}$ and $\bar{\theta}_{l1}$ of the l-th $(l=1,2,\ldots,L)$ cell and take them as the two downtilts of the l-th cell.

4.1 Problem Formulation

Based on the analysis above, joint optimization problem is formulated as

$$\max_{(\mathbf{w}_{l0},\mathbf{w}_{l1},P_{l0},P_{l1})} f=\sum_{l=1}^{L}\left(\sum_{k_0=1}^{K'}R_{lk_0}+\sum_{k_1=1}^{K'}R_{lk_1}\right) \tag{14}$$

$$s.t. \quad C1:\left\|\mathbf{w}_{l0}^{H}\right\|^2=\left\|\mathbf{w}_{l1}^{H}\right\|^2=1,\ \rho_l\le\rho_{\max},C2:P_{l0}+P_{l1}=P,(\forall l\in\{1,2,\ldots,L\})$$

The inter-sector correlation coefficient ρ is defined by [18]:

$$\rho=\frac{\int_{-\pi}^{\pi}\left(\mathbf{w}_{l0}^{H}\mathbf{B}r\left(\theta,\bar{\theta}_{D,l0}\right)\right)\left(\mathbf{w}_{l1}^{H}\mathbf{B}r\left(\theta,\bar{\theta}_{D,l1}\right)\right)^{*}p(\theta)d\theta}{\int_{-\pi}^{\pi}\left|\mathbf{w}_{l0}^{H}\mathbf{B}r\left(\theta,\bar{\theta}_{D,l0}\right)\right|^2p(\theta)d\theta\int_{-\pi}^{\pi}\left|\mathbf{w}_{l1}^{H}\mathbf{B}r\left(\theta,\bar{\theta}_{D,l1}\right)\right|^2p(\theta)d\theta}, \tag{15}$$

where $p(\theta)$ is the distribution of the users' elevation angles.

In the optimization problem, in order to suppress the inter-sector interference, we consider the constraint of inter-sector correlation. The limitation C1 indicates an upper bound on the inter-sector correlation and guarantees the power unchanged in adjusting the weight vectors of antennas. The limitation C2 indicates the power constraint of base station.

4.2 Vertical Beams optimization based on PSO Algorithm

The optimization problem (14) is a constrained non-convex problem with multiple multidimensional variables. A traditional optimization method is to alternately and iteratively allocate the power with fixed weight vectors by applying the Karush-Kuhn-Tucker (KKT) condition and adjust the weight vectors with fixed powers of beams. This traditional algorithm calls for unacceptable complexity. In order to efficiently solve the joint adaptation problem in (14), some suboptimal approaches such as particle swarm optimization (PSO) optimization algorithm in [15] can be applied. The PSO based

optimization algorithm for problem (14) is described as the following procedure:

Step 1: Initialize the velocity and location of particles according to the constraint of each variable. We initialize the velocity and location of the *j*-th particle of power in *l*-th cell as

$$v_{P_{li}}^{j}(1)=P\times\varepsilon-\frac{P}{2},\ P_{li}^{j}(0)=\frac{P}{2},\quad i\in\{0,1\} \tag{16}$$

Initialize the velocity and location of the *j*-th particle of $\mathbf{w}_1$'s and $\mathbf{w}_2$'s $[(n-1)N_v+m]$-th elements in *l*-th cell as

$$\begin{cases} v_{w_{l0}}^{j}(1)=(\frac{\varepsilon}{2}-1)\cos[\frac{2\pi}{\lambda}(d_y m\sin\bar{\theta}_{l0}+d_z n\cos\bar{\theta}_{l0})]-(\frac{\varepsilon}{2}-1)j\sin[\frac{2\pi}{\lambda}(d_y m\sin\bar{\theta}_{l0}+d_z n\cos\bar{\theta}_{l0})] \\ w_{l0,m,n}^{j}(0)=\cos[\frac{2\pi}{\lambda}(d_y m\sin\bar{\theta}_{l0}+d_z n\cos\bar{\theta}_{l0})]-j\sin[\frac{2\pi}{\lambda}(d_y m\sin\bar{\theta}_{l0}+d_z n\cos\bar{\theta}_{l0})] \end{cases} \tag{17}$$

and

$$\begin{cases} v_{w_{l1}}^{j}(1)=(\frac{\varepsilon}{2}-1)\cos[\frac{2\pi}{\lambda}(d_y m\sin\bar{\theta}_{l1}+d_z n\cos\bar{\theta}_{l1})]-(\frac{\varepsilon}{2}-1)j\sin[\frac{2\pi}{\lambda}(d_y m\sin\bar{\theta}_{l1}+d_z n\cos\bar{\theta}_{l1})] \\ w_{l1,m,n}^{j}(0)=\cos[\frac{2\pi}{\lambda}(d_y m\sin\bar{\theta}_{l1}+d_z n\cos\bar{\theta}_{l1})]-j\sin[\frac{2\pi}{\lambda}(d_y m\sin\bar{\theta}_{l1}+d_z n\cos\bar{\theta}_{l1})], \end{cases} \tag{18}$$

respectively, where $\varepsilon\in U(0,1)$ and $j=1,2,\ldots,S$ is the index of the particle. *S* denotes the number of the particles in a swarm.

Step 2: (a)Update the velocity and location of each particle according to the PSO update formulas [15]:

$$\begin{cases} v_x^j(\tau)=av^j(\tau-1)+c_1r_1[p_x^j(\tau-1)-x^j(\tau-1)]+c_2r_2[p_x^g(\tau-1)-x^g(\tau-1)] \\ x^j(\tau)=x^j(\tau-1)+v_x^j(\tau) \end{cases} \tag{19}$$

where r_1 and r_2 are random numbers following the uniform distribution between 0 and 1. c_1 and c_2 are the learning factors. a is the inertia factor (In the simulation, we set $a=1.2-0.4\times Iterationindex/MaximumIterations$ [19]). p_x^j is the local optimum position of particles and p_x^g is the global optimum position of particles. x^j and v_x^j are the position and velocity of *j*-th particle of the variable *x*, respectively. τ denotes the τ-th iteration;

(b)Judge whether $\mathbf{w}_{l0}^j(\tau)$ and $\mathbf{w}_{l1}^j(\tau)$ meet the conditions of correlation. If not, change the value of ε in (17) and (18), then update $\mathbf{w}_{l0}^j(\tau)$ and $\mathbf{w}_{l1}^j(\tau)$ according to (19) until the conditions are met. Judge whether $P_{li}^j(\tau)$ is within its range. If it exceeds the range, let $v_{P_{li}}^j(\tau)=v_{P_{li}}^j(\tau)/2$ and then update $P_{li}^j(\tau)$ again.

(c)Set the cluster spectral efficiency *f* to be the fitness function. Then compare the values of all fitness functions got from all previous iterations and obtain the local optimum position $p_x^j(\tau)$, the global optimum position $p_x^g(\tau)$ of each variable and the global optimum value of the fitness function, i.e. f_m^τ.

(d)If the maximal iteration is reached or $[f_m^\tau-f_m^{\tau-1}]<\delta$,where δ is a small constant, the iteration is stopped. Otherwise set $\tau=\tau+1$ and go to step (b).

4.3 Complexity Analysis

In this section, the complexity of our downlink optimization algorithm is analyzed. In each iteration, calculating the antenna gains of all users needs a complexity of $o(2LK' \cdot 2L \cdot M^2)$ and calculating the SINR of all users needs a complexity of $o((2LK')^2 \cdot M^2)$. So calculating the cluster spectral efficiency of all particles results a complexity of $o(S[(2L)^2 K' + (2LK')^2]M^2)$. In our scheme, $2L \cdot (M+1)$ variables are needed to be optimized, so the complexity of updating the locations and velocities of the particles is $o(2L(M+1)S)$. Therefore, the complexity of the proposed algorithm is $o(2L(M+1)S) + o(S[(2L)^2 K' + (2LK')^2]M^2)$, which is higher than the algorithm proposed in [12] with the complexity of $o(SM^2)$. But with our algorithm, the system performance could be improved significantly. When the number of antennas is much larger than L and K', the complexity of the proposed downlink scheme increases linearly compared with the algorithm in [12].

5. Simulation Results and Discussions

In the simulation, system level performances of the proposed optimal schemes are evaluated. The performance indicators include channel estimation MSE in uplink and cell average spectral efficiency in downlink. One coordination cluster with 7 cells, each of which is divided into two vertical sectors, is studied in our simulation. In addition, the number of horizontal antennas of UPA remains $N_t = 4$ with the total number of antennas increasing in the simulation. *K* users are placed randomly in each cell.

In 3D MIMO systems, a 3D channel model is more realistic. So a simplified 3D spatial channel model based on finite scattering physical channel modelling is adopted in our simulation. This simplified 3D spatial channel model is directly extended from the 2D physical channel model [7] by introducing the vertical AOA spread of propagation paths.

Assume that there are *U* independent paths between a user and a base station. The channel coefficient between an user and the *m*-th antenna of a base station is written as

$$h_m = \frac{1}{\sqrt{U}} \left(\sum_{u=1}^{U} e^{-j\frac{2\pi D}{\lambda}\left[\cos(\theta_u),\ \sin(\theta_u)\sin(\varphi_u)\right](\mathbf{u}_m - \mathbf{u}_1) - j\phi_u} g_u \right), \tag{20}$$

where θ_u and φ_u are the vertical and horizontal AOA of the *u*-th path. It is assumed that θ_u and φ_u both follow the complex Gaussian distribution. There are $\theta_u \backsim CN(\overline{\theta}, \sigma_\theta^2)$ and $\varphi_u \backsim CN(\overline{\varphi}, \sigma_\varphi^2)$, where σ_θ and σ_φ are the vertical AOA spread and the horizontal AOA spread, respectively. Moreover, ϕ_u is the phase of the *u*-th path and $\phi_u \backsim U(-\pi, \pi)$. g_u is the i.i.d $CN(0,1)$ random variable and $\mathbf{u}_m \in R^{2\times 1}$ is the location vector of *m*-th antenna element in UPA. In addition, *D* is the distance between the two adjacent antenna elements both in vertical and horizontal dimension.

From (20), we can obtain the correlation coefficient between the *m*-th antenna and the *p*-th antenna of antenna array, which is calculated as

$$\begin{aligned}\left[\mathbf{R}\right]_{m,p} &= E\left\{h_m h_p^*\right\} \\ &= \frac{1}{2\pi\sigma_\theta\sigma_\varphi}\int_{-\infty}^{+\infty}\int_{-\infty}^{+\infty} e^{-j\frac{2\pi D}{\lambda}\left(\cos(\theta),\sin(\theta)\sin(\varphi)\right)\left(\mathbf{u}_m-\mathbf{u}_p\right)-\frac{(\theta-\bar{\theta})^2}{2\sigma_\theta^2}-\frac{(\varphi-\bar{\varphi})^2}{2\sigma_\varphi^2}} d\theta d\varphi\end{aligned} \tag{21}$$

Based on (21), we can obtain the channel covariance matrix $\mathbf{R}_{jlk}$ in Section 2.1. While, in our proposed uplink and downlink schemes, it is not needed to calculate Eq.(21) since $\mathbf{R}_{jlk}$ is not used directly.

Some basic simulation parameters are listed in **Table 1**.

Table 1. Basic simulation parameters

Parameters	Assumptions
Channel model	refer to part 1 of section 2
Cell radius	1000m
Base station height and UE height	BS:32m; UE:1.5m
Antenna spacing	Vertical:0.5 λ , Horizontal:0.5 λ
Pass loss exponent	3
Vertical HPBW	6.5°
Pilot and Data SNR	5dB and 20dB
Coherence interval	18 symbols
$\sigma_\theta, \sigma_\varphi$	4° , 10°

The normalized MSE of channel estimation is used to evaluate the proposed scheme in section 3, which can be expressed as

$$err = 10\lg E\{(\sum_{j=1}^{L}\sum_{k=1}^{K}\left\|\hat{\mathbf{b}}_{jjk}-\mathbf{b}_{jjk}\right\|_F^2)/(\sum_{j=1}^{L}\sum_{k=1}^{K}\left\|\mathbf{b}_{jjk}\right\|_F^2)\} \tag{22}$$

Besides, the cell average spectral efficiency written as (23) is used to assess the downlink performance.

$$C=\sum_{j=1}^{L}(\sum_{i_0=1}^{K'}R_{ji_0}+\sum_{i_1=1}^{K'}R_{ji_1})/L \tag{23}$$

5.1 Uplink Performance

In **Fig. 2**, we compare the normalized MSE of channel estimation with different pilot reuse factor, where no optimization is executed. Here, the non-orthogonal pilot sequences are reused across cells in traditional massive MIMO system, and the pilot reuse factor is $r=1$ for this case. While, in 3D massive MIMO system, the non-orthogonal pilots are reused fully or partially across vertical sectors where the corresponding pilot reuse factor is $r=0.5$ or $r=5/6$. It can be seen from **Fig. 2** that the normalized MSE of channel estimation increases as the pilot reuse factor grows. This is because that the larger pilot

reuse factor is, the more users assigned with same pilot sequences would be in a cell, then the pilot contamination is more serious. This result is consistent with the analysis in section 3.

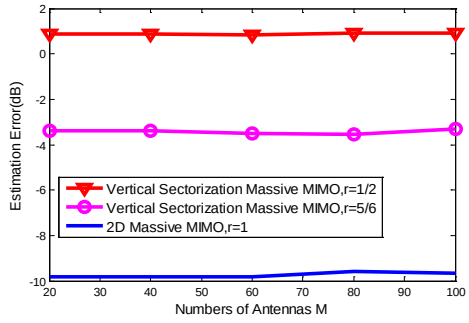

Fig. 2. Channel estimation error without optimization

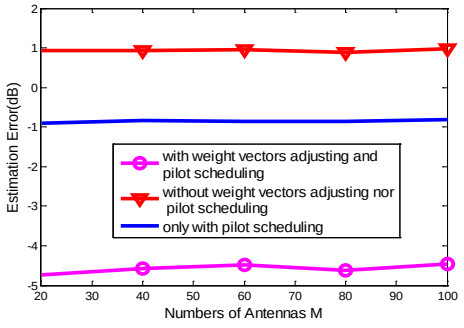

Fig. 3. Channel estimation error with pilot scheduling and weight vector adjustment, $r = 0.5$

The effect of the proposed scheme is shown in **Fig. 3**, where the worst case of pilot contamination with $r = 0.5$ is focused on. It could be seen that if the pilot scheduling is executed only, the channel estimation error reduced in some degree. And if the weight vectors of vertical beams are adjusted in conjunction with pilot scheduling the channel estimation error could be reduced further. From **Fig. 3**, we can see that a gain of more than 5dB is obtained by the proposed joint optimization scheme for uplink. On the other hand, we could see that the MSE of LS channel estimation almost doesn't change with the number of antennas, and the same result could be seen in [7]. The main reason is as follows. Firstly, the LS channel estimation according to each receiver antenna is actually executed parallel and independently. Furthermore, when M increases, the transmission power of the user's pilot, the pilot reuse factor and other system parameters all keep invariant, so the received pilot SINR of each antenna for LS estimation doesn't change. Therefore, the LS estimation error does not depend on the number of antennas.

The impact of our uplink joint optimization scheme on the downlink performance would be displayed in the next part.

5.1 Downlink Performance

In order to assess the performance of the proposed downlink joint optimization approach and the effect of the uplink design in section 3 on the downlink data transmission, the downlink cell average spectral efficiency versus the number of antennas is investigated. There are four scenarios simulated for comparison: (1) 2D massive MIMO system: Vertical sectorization is not included in a cell and traditional 2D MU-MIMO precoding is used in downlink and LS channel estimation is used in uplink. (2) 3D massive MIMO system with two vertical beams having fixed downtilts and equal powers in a cell for downlink: The two downtilts of two vertical sectors are fixedly selected as the average elevation angles of users within two sectors. And the beam power is equal for each vertical sector. (3) 3D massive MIMO system with two vertical beams having adaptive downtilts and powers in a

cell for downlink [12]. The difference from [12] is that the estimated CSI being used in our simulation. (4) 3D massive MIMO system adopting only the proposed design for downlink in section 4 (For this case, the traditional un-optimized uplink scheme is used.) or the both designs for uplink and downlink of ours.

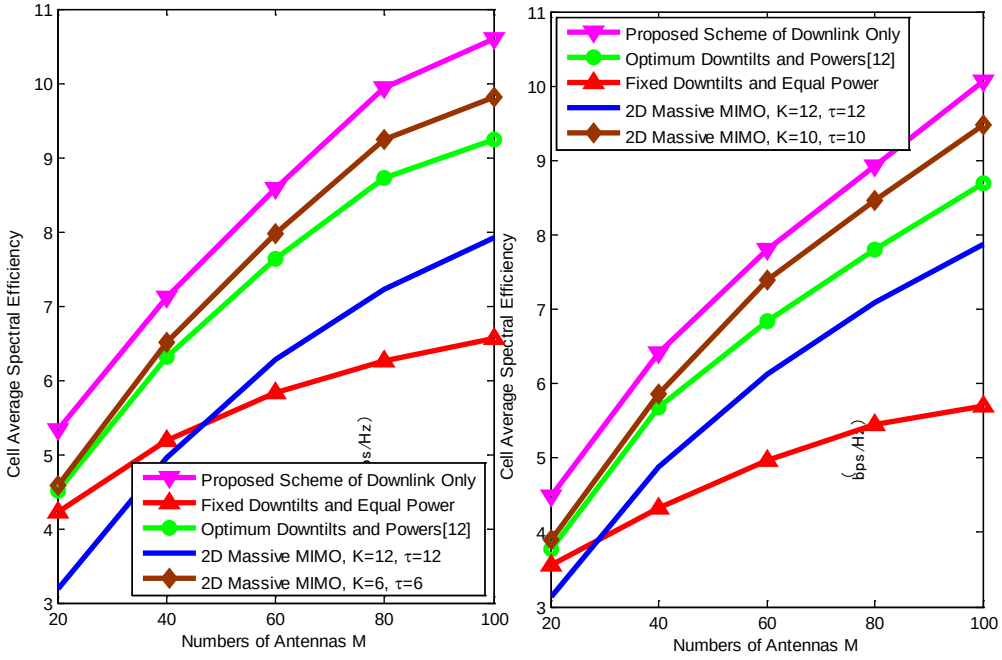

(a) $r = 0.5$ (b) $r = 5/6$

Fig. 4. Cell average spectral efficiency with the traditional un-optimized uplink scheme

Fig. 4(a) displays the cell average spectral efficiency under four scenarios, where the traditional uplink scheme is considered for all of the 3D massive MIMO designs. Moreover, for **the** 3D massive MIMO case, the number of users in each cell is K=12 and the length of pilot sequence is $\tau = 6$, i.e. $r = 0.5$. For 2D massive MIMO, we consider two cases, K=12 , τ =12 and K=6 , $\tau = 6$.

Firstly, we observe that the cell average spectral efficiency of all scenarios increases as the number of antennas grows, because the influence of uncorrelated interferences is eliminated gradually with the increase of antennas. But the existing pilot contamination limits the growth of cell average spectral efficiency and the performance improvement for various cases becomes slow as M increases. It is a good agreement with the theoretical analysis in [3]. Secondly, the performance of two 3D scenarios with optimization is far better than 2D scenario when the number of users in each cell is the same (K=12). There are two main reasons for this. The first reason is that there are more time resources to transmit users' information data with the length of pilot sequence in 3D system being 6 rather than 12 in 2D system. The other one is the two optimized 3D system design could coordinate the inter-cell and intra-cell interference effectively by adjusting the system

parameters adaptively, such as the downtilt, weight vector and power of each beam. Furthermore, the optimization of system parameters has greater contribution to the performance improvement. Because the benefit of low pilot overhead in the 3D scenario with fixed downtilts and equal powers reduces gradually when the number of antennas increases. Especially, the 3D system with fixed downtilts and equal powers will be worse than the traditional 2D scenario for M being larger than 50, although the former has lower pilot overhead. The reason is that the pilot contamination in 3D system is more serious, meanwhile, the pilot contamination would become the major limiting factor with large number of antenna. Moreover, the downlink algorithm we proposed could control the vertical beam more precisely, so better system performance is got. Specifically, the proposed downlink algorithm obtains a gain of more than 2bps/Hz against the 2D scenario. Thirdly, we also give the cell average spectral efficiency of 2D scenario with K=6 and $\tau = 6$ in **Fig. 4(a)**. Compared with 2D scenario with K=12 and $\tau = 12$, the performance is improved although the number of users reduce to the half. That is because **of** the lower pilot overhead and the less inter-user interference. Moreover, compared with two 3D scenarios, including scenario (2) and scenario (3), the performance of the 2D scenario with K=6 and $\tau = 6$ is also better, although they have the same pilot overhead and more users are served by 3D systems. That is because more serious pilot contamination and inter-user interference exist in 3D scenarios. While, thanks for the more precise interference coordination, the proposed joint optimization scheme still outperforms the 2D system with K=6 and $\tau = 6$.

In order to analyze the trade-off problem between the pilot overhead and pilot contamination, the cases of $r = 5/6$ is simulated further. Here, the number of users in a cell for 3D scenarios remains as K=12. That is to say the pilot overhead increases with the r growing. From **Fig. 4(b)** and **Fig. 4(c)**, we can see that the cell average spectral efficiency of all the 3D systems decreases with r increasing. The result shows that although the increase of r would induce the lower pilot contamination, the performance loss caused by high pilot overhead is relatively larger. On the other hand, we can also see from **Fig. 4(b)** that although the users served by a base station increases, the system performance still decreases because of higher pilot overhead in 2D scenario with $K = 10$ and $\tau = 10$. Of course, the above results would also depend on the coherence time length. Nevertheless, they remind us that the trade-off problem between the pilot overhead and pilot contamination should be considered carefully when we select the number of served users per cell and the length of pilot sequence in 3D vertical sectorization scenario.

Fig. 5 shows the CDF of capacity per user for four scenarios with the traditional uplink scheme, where K=12 and M=100. For 3D scenarios, $\tau = 6$ and $r = 0.5$. While, for 2D scenario, $\tau = 12$ and $r = 1$. It can be seen that the proposed downlink scheme has the highest capacity per user among the three 3D scenarios, since it could reduce the various interference efficiently by adjusting the beams' weight vectors and limiting the inter-sector correlation. Moreover, in comparison to the 2D system, the edge users have worse performance and more users have low spectrum efficiency in the three 3D systems. On the contrary, sector-center users of 3D systems have better performance than the cell-center

users in 2D scenario. At last, the cell average spectral efficiency in 3D systems is higher (seen from **Fig. 4(a)**). This result is related to the influence of vertical beam's HPBW. Limited by the HPBW of the vertical beam, if a user lies near the center directions of vertical beams, this user would receive higher signal power, otherwise it's received signal power is lower. At the same time, the sector-center users lying at the center area covered by some vertical beam would undergo slight interference, while the sector-edge users far from the main direction of any vertical beam would bear serious interference. So it leads to the result of **Fig. 5**. The performance imbalance between sector-edge users and sector-center users is a key problem in vertical sectorization system. In order to solve this problem, a scheme combining multi-cell downlink joint transmission with 3D beamforming in cell edge is proposed in [16], and a method that orthogonal resource blocks are allocated to the sector-edge users and sector-center users is studied in [17].

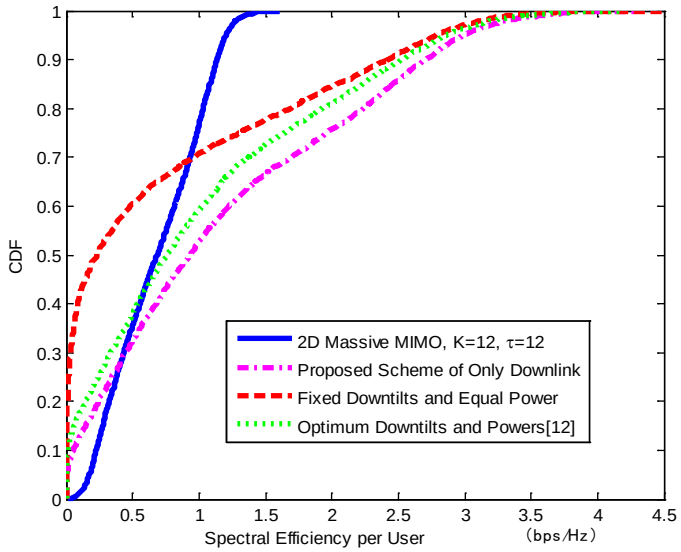

Fig. 5. CDF of the spectral efficiency per user for four scenarios with the traditional uplink scheme. Here, $r = 0.5$ for 3D cases and $M = 100$.

The effect on the downlink cell average spectral efficiency of the proposed joint weight vectors adjustment and pilot scheduling in uplink is shown in **Fig. 6(a)** and **Fig. 6(b)**. With the proposed uplink optimization scheme, more serious pilot contamination caused by vertical sectorization is suppressed and channel estimation error is reduced. And the downlink throughput of the system using the channel estimates of our uplink scheme is improved significantly. Moreover, the scenario with more serious pilot contamination obtains the larger performance gain through using the proposed uplink optimization design.

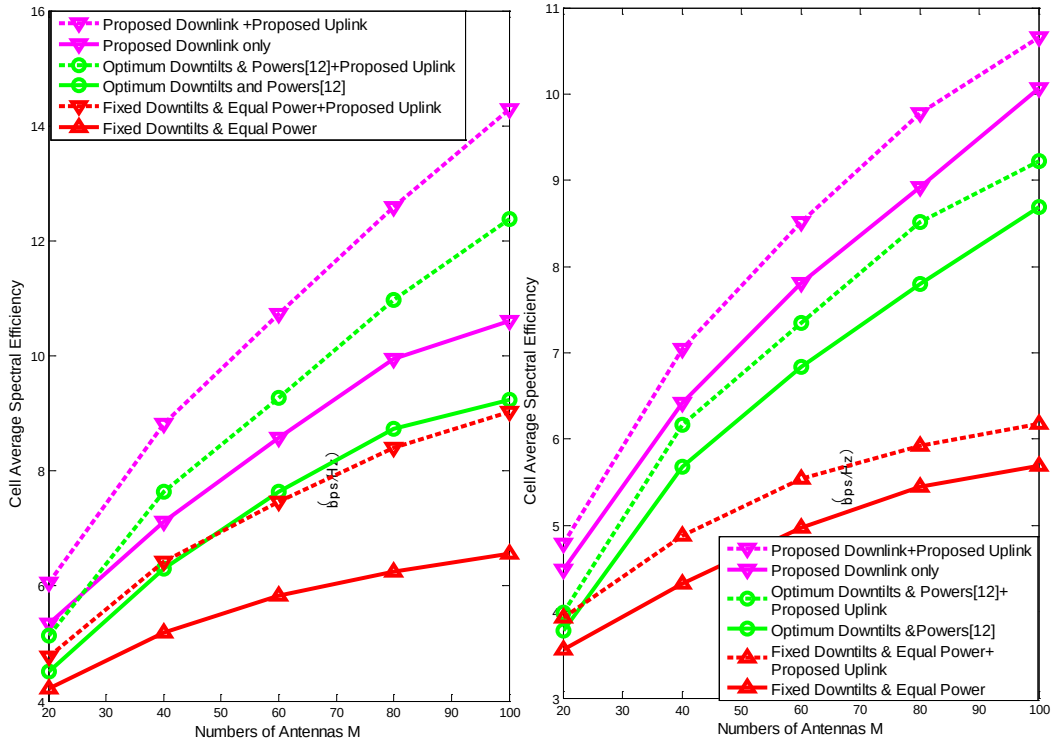

(a) $r = 0.5$ (b) $r = 5/6$

Fig. 6. Cell average spectral efficiency with the proposed uplink scheme.

5. Conclusions

In this paper, we investigate interference management in 3D massive MIMO systems with vertical sectorization based on vertical beamforming. In the uplink, iterative weight vectors adjustment for vertical beams and pilot scheduling are applied to improve the accuracy of channel estimation. In the downlink, an adaptive joint weight vectors adjustment and power allocation scheme for vertical beams is proposed to coordinate the interferences among sectors and cells. The simulation results show that the proposed downlink optimization algorithm to adjust the weight vectors of vertical beams outperforms the downtilts adjustment based method. When the channel estimates obtained by our uplink scheme are used to transmit the downlink data, the downlink cell spectral efficiency could be improved further. However, the complexity of the proposed joint optimization methods based on PSO algorithm is still too high for realization. And a more simple solving method will be investigated in our future work.

Appendix

We now give the derivation of the average SINR when $M \to \infty$. From (9), we can get the available signal power of the i_0-th user in the near sector of the j-th cell is

$$\lim_{M\to\infty} E\left\{\left|\mathbf{g}_{ji_0}^{j0}\mathbf{a}_{jji_0}\right|^2\right\} = P_{j0}A(\theta_{D,j0},\theta_{jji_0})_d \lim_{M\to\infty} E\{\left|\mathbf{b}_{jji_0}^T \frac{\hat{\mathbf{b}}_{jji_0}^*}{a_{jji_0}\sqrt{M}}\right|^2\} \tag{24}$$

When we analysis the pilot contamination in our assume system, the following well known Lemma will be useful for us.

Lemma 1: Let $\mathbf{x},\mathbf{y} \in C^{M\times 1}$ be two independent vectors with the distribution of $CN(0,c\mathbf{I})$, then

$$\lim_{M\to\infty} \frac{\mathbf{x}^H\mathbf{y}}{M} \overset{a.s.}{=} 0 \; and \; \lim_{M\to\infty} \frac{\mathbf{x}^H\mathbf{x}}{M} \overset{a.s.}{=} c \tag{25}$$

So

$$\begin{aligned}&\lim_{M\to\infty} E\left\{\left|\mathbf{b}_{jji_0}^T\hat{\mathbf{b}}_{jji_0}^*\right|^2\right\}\\ &= \lim_{M\to\infty} E\left\{\left|\mathbf{b}_{jji_0}^T\mathbf{b}_{jji_0}^*\right|^2 + \left|\mathbf{b}_{jji_0}^T\mathbf{b}_{jji_1}^* \frac{\sqrt{A(\theta_{D,j0},\theta_{jji_1})_u}}{\sqrt{A(\theta_{D,j0},\theta_{jji_0})_u}}\right|^2 + \left|\sum_{l=1,l\neq j}^{L}\sum_{n=0}^{1}\mathbf{b}_{jji_0}^T\mathbf{b}_{jli_n}^* \frac{\sqrt{A(\theta_{D,j0},\theta_{jli_n})_u}}{\sqrt{A(\theta_{D,j0},\theta_{jji_0})_u}}\right|^2 + \left|\frac{\mathbf{z}_l^*\Psi_k^H}{\tau\sqrt{p_r A(\theta_{D,j0},\theta_{jji_0})_u}}\right|^2\right\}\end{aligned} \tag{26}$$

where

$$\lim_{M\to\infty} E\left\{\mathbf{b}_{jji_0}^T\mathbf{b}_{jji_0}^*\right\} = \beta_{jji_0} tr\left\{\mathbf{R}_{jji_0}\right\} = M\beta_{jji_0},$$

$$\lim_{M\to\infty} E\left\{\mathbf{b}_{jji_0}^T\mathbf{b}_{jji_1}^*\right\} = 0,$$

$$\lim_{M\to\infty} E\left\{\left|\mathbf{b}_{jji_0}^T\mathbf{b}_{jji_1}^*\right|^2\right\} = \beta_{jji_0}\beta_{jji_1} tr\left\{\mathbf{R}_{jji_1}^{1/2}\mathbf{R}_{jji_0}\mathbf{R}_{jji_1}^{1/2}\right\}.$$

In a massive MIMO system, we consider that $M^2 >> M$. Furthermore, all elements on the primary diagonal of $\mathbf{R}_{jji}$ are 1and the other elements are less than 1. Then, we can get $M^2 >> tr\left\{R_{jji}^2\right\}$.So the above equation can be written as,

$$\begin{aligned}&\beta_{jji_0}^2 M^2 + \frac{A(\theta_{D,j0},\theta_{jji_1})_u}{A(\theta_{D,j0},\theta_{jji_0})_u}\beta_{jji_0}\beta_{jji_1} tr\left\{\mathbf{R}_{jji_1}^{1/2}\mathbf{R}_{jji_0}\mathbf{R}_{jji_1}^{1/2}\right\}\\ &+ \sum_{l=1,l\neq j}^{L}\sum_{n=0}^{1}\frac{A(\theta_{D,j0},\theta_{jli_n})_u}{A(\theta_{D,j0},\theta_{jji_0})_u}\beta_{jji_0}\beta_{jli_n} tr\left\{\mathbf{R}_{jji_0}^{1/2}\mathbf{R}_{jli_n}\mathbf{R}_{jji_0}^{1/2}\right\} + \frac{KM\beta_{jji_0}}{\tau^2 p_r A(\theta_{D,j0},\theta_{jji_0})_u} \approx \beta_{jji_0}^2 M^2\end{aligned} \tag{27}$$

So (24) can be expressed as

$$\lim_{M\to\infty}\frac{1}{M}E\left\{\left|\mathbf{g}_{ji_0}^{j0}\mathbf{a}_{jji_0}\right|^2\right\} \approx P_{j0}A(\theta_{D,j0},\theta_{jji_0})_d \frac{\beta_{jji_0}^2}{a_{jji_0}^2}, \tag{28}$$

where

$$\lim_{M\to\infty} a_{jji_0}^2 = \beta_{jji_0} + \frac{\sqrt{A(\theta_{D,j0},\theta_{jji_1})_u}}{\sqrt{A(\theta_{D,j0},\theta_{jji_0})_u}}\beta_{jji_1} + \sum_{l=1,l\neq j}^{L}\sum_{n=0}^{1}\frac{\sqrt{A(\theta_{D,j0},\theta_{jli_n})_u}}{\sqrt{A(\theta_{D,j0},\theta_{jji_0})_u}}\beta_{jli_n} + \frac{K}{\tau^2 p_r A(\theta_{D,j0},\theta_{jji_0})_u} \tag{29}$$

Similarly, the average power of intra-sector interference can be expressed as

$$\begin{aligned}
&\lim_{M\to\infty}\frac{1}{M}E\left\{\sum_{k_0=1,k_0\neq i_0}^{K'}\left|\mathbf{g}_{ji_0}^{j0}\mathbf{a}_{jjk_0}\right|^2\right\}\\
&= P_{j0}A(\theta_{D,j0},\theta_{jji_0})_d\sum_{k_0=1,k_0\neq i_0}^{K'}\frac{\beta_{jji_0}}{M^2 a_{jjk_0}^2}[\beta_{jjk_0}tr\left\{\mathbf{R}_{jjk_0}^{1/2}\mathbf{R}_{jji_0}\mathbf{R}_{jjk_0}^{1/2}\right\}\\
&+\frac{\beta_{jjk_1}tr\left\{\mathbf{R}_{jjk_1}^{1/2}\mathbf{R}_{jji_0}\mathbf{R}_{jjk_1}^{1/2}\right\}A(\theta_{D,j0},\theta_{jjk_1})_u}{A(\theta_{D,j0},\theta_{jjk_0})_u}\\
&+\sum_{\substack{l=1\\l\neq j}}^{L}\sum_{n=0}^{1}\frac{\beta_{jlk_n}tr\left\{\mathbf{R}_{jlk_n}^{1/2}\mathbf{R}_{jji_0}\mathbf{R}_{jlk_n}^{1/2}\right\}A(\theta_{D,j0},\theta_{jlk_n})_u}{A(\theta_{D,j0},\theta_{jjk_0})_u}+\frac{K}{\tau^2 p_r A(\theta_{D,j0},\theta_{jjk_0})_u}]\\
&\approx 0
\end{aligned} \tag{30}$$

The average power of inter-sector interference can be expressed as

$$\begin{aligned}
&\lim_{M\to\infty}\frac{1}{M}E\left\{\sum_{k_1=1}^{K'}\left|\mathbf{g}_{ji_0}^{j1}\mathbf{a}_{jjk_1}\right|^2\right\}\\
&=\lim_{M\to\infty}\frac{P_{j1}A(\theta_{D,j1},\theta_{jji_0})_d}{M}E\left\{\left|\mathbf{b}_{jji_0}^T\frac{\hat{\mathbf{b}}_{jji_1}^*}{a_{jji_1}\sqrt{M}}\right|^2+\sum_{k_1=1,k_1\neq i_1}^{K'}\left|\mathbf{b}_{jji_0}^T\frac{\hat{\mathbf{b}}_{jjk_1}^*}{a_{jjk_1}\sqrt{M}}\right|^2\right\}\\
&\approx P_{j1}A(\theta_{D,j1},\theta_{jji_0})_d\frac{\beta_{jji_0}^2}{a_{jji_1}^2}\frac{A(\theta_{D,j1},\theta_{jji_0})_u}{A(\theta_{D,j1},\theta_{jji_1})_u}
\end{aligned} \tag{31}$$

The average power of inter-cell interference can be expressed as

$$\begin{aligned}
&\lim_{M\to\infty}\frac{1}{M}E\left\{\sum_{k_1=1}^{K'}\left|\mathbf{g}_{ji_0}^{j1}\mathbf{a}_{jjk_1}\right|^2\right\}\\
&=\lim_{M\to\infty}\frac{P_{j1}A(\theta_{D,j1},\theta_{jji_0})_d}{M}E\left\{\left|\mathbf{b}_{jji_0}^T\frac{\hat{\mathbf{b}}_{jji_1}^*}{a_{jji_1}\sqrt{M}}\right|^2+\sum_{k_1=1,k_1\neq i_1}^{K'}\left|\mathbf{b}_{jji_0}^T\frac{\hat{\mathbf{b}}_{jjk_1}^*}{a_{jjk_1}\sqrt{M}}\right|^2\right\}\\
&\approx P_{j1}A(\theta_{D,j1},\theta_{jji_0})_d\frac{\beta_{jji_0}^2}{a_{jji_1}^2}\frac{A(\theta_{D,j1},\theta_{jji_0})_u}{A(\theta_{D,j1},\theta_{jji_1})_u}
\end{aligned} \tag{32}$$

Then, using (28), (30), (31) and (32), we have the approximate SINR expression in (11).

References

[1] Guangen Wu, Pinyi Ren, Qinghe Du, "Recall-Based Dynamic Spectrum Auction with the Protection of Primary Users," *Selected Areas in Communications IEEE Journal on 30.10 (2012)*, 2070-2081, 2012. Article (CrossRef Link)

[2] Wenshan Yin, Pinyi Ren, Zhou Su, Ruijuan Ma, "A Multiple Antenna Spectrum Sensing Scheme Based on Space and Time Diversity in Cognitive Radios," *Ieice Transactions on Communications 94.5(2011)*, 1254-1264, 2011. Article (CrossRef Link)

[3] T. L. Marzetta, "Noncooperative cellular wireless with unlimited numbers of base station antennas," *IEEE Transactions on Wireless Communications*, Vol. 9, Issue: 11, pp. 3590-3600, 2010. Article (CrossRef Link)

[4] P Ren, Y Wang, Q Du, "CAD-MAC: A Channel-Aggregation Diversity Based MAC Protocol for Spectrum and Energy Efficient Cognitive Ad Hoc Networks," *Selected Areas in Communications IEEE Journal on 32.2(2014)*, 237–250, 2014. Article (CrossRef Link)

[5] J. Jose, A. Ashikhmin, T. L. Marzettaet et al., "Pilot contamination problem in multi-cell TDD systems," in *Proc. of IEEE International Symposium on Information Theory (ISIT09)*. Seoul, Korea, pp. 2184-2188, 2009. Article (CrossRef Link)

[6] H. Q. Ngo, E. G. Larsson, "EVD-Based Channel Estimation in Multicell Multiuser MIMO Systems with Very Large Antenna Arrays," in *Proc. of 2012 IEEE International Conference on Acoustics, Speech and Signal Processing (ICASSP)*, pp.3249-3252, March 2012. Article (CrossRef Link)

[7] Haifan Yin, D. Gesbert, M. Filippou, et al., "A Coordinated Approach to Channel Estimation in Large-scale Multiple-antenna Systems," *IEEE Journal on Selected Areas in Communications*, Vol.31, No.2, pp.264-273, January 2013. Article (CrossRef Link)

[8] A. Ashikhmin, T. L. Marzetta, "Pilot Contamination Precoding in Multi-Cell Large Scale Antenna Systems," in *Proc. of 2012 IEEE international Symposium on Information Theory Proceedings (ISIT)*, pp.1137-1141, July 2012. Article (CrossRef Link)

[9] F. Fernandes, A. Ashikhmin, T. L. Marzetta, "Inter-Cell Interference in Noncooperative TDD Large Scale Antenna Systems," *IEEE Journal on Selected Areas in Communications*, Vol.31, No.2, pp.192-201, February 2013. Article (CrossRef Link)

[10] Yan Li, Xiaodong Ji, Mugen Peng, et al., "An Enhanced Beamforming Algorithm for Three Dimensional MIMO in LTE-Advanced Networks," in *Proc. of Wireless Communications Signal Processing (WCSP), 2013 International Conference on*, pp. 1-5, 2013. Article (CrossRef Link)

[11] M.Caretti, M.Crozzoli. G.M. DellAera, et al., "Cell Splitting Based on Active Antennas: Performance Assessment for LTE system," in *Proc. of Wireless and Microwave Technology Conference (WAMICON), 2012 IEEE 13th Annual*, Page(s) :1-5, 2012. Article (CrossRef Link)

[12] YayingWu, Xiaohui Li, Yongqiang Hei, "Downtilts adjustment and power allocation algorithm based on PSO for 3D MIMO systems," in *Proc. of Information and Communications Technologies (IETICT 2013), IET International Conference on*, Page(s): 557-563, 2013. Article (CrossRef Link)

[13] Zhang, W., Wang, Y., Peng, F., et al., "Interference Coordination with Vertical Beamforming in 3D MIMO-OFDMA Networks," *Communications Letters*, IEEE, Page(s):1-4, 2013. Article (CrossRef Link)

[14] Tomoki Murakami, Riichi Kudo, Koichi Ishihara, et al., "Cooperative Interference Management by Beam Tilt and Power Controls in an Indoor Muti-Cell Environment," in *Proc. of 2013 7th European Conference on Antennas and Propagation (EuCAP)*, Page(s): 643-647,

2013. Article (CrossRef Link)
[15] J. Kennedy, R. Eberhart, "Particle Swarm Optimization," in *Proc. of* the *IEEE International Conference on Neural Networks*, pp. 1942-1948, 1995. Article (CrossRef Link)
[16] Hong Zhu, Ying Wang, Cong Shi, et al., "Multi-cell Downlink Joint Transmission with 3D Beamforming," in *Proc. of Vehicular Technology Conference (VTC Fall), 2013 IEEE 78th*, Page(s): 1 – 5, 2013. Article (CrossRef Link)
[17] Chang-Shen Lee, Ming-Chun Lee, Chung-Jung Huang, et al., "Sectorization with Beam Pattern Design Using 3D Beamforming Techniques," in *Proc. of Signal and Information Processing Association Annual Summit and Conference (APSIPA)*, 2013 Asia-Pacific, Page(s): 1 – 5, 2013. Article (CrossRef Link)
[18] Tsakalaki, E.P., de Temino, L.A.M.R., et al., "Deterministic Beamforming for Enhanced Vertical Sectorization and Array Pattern Compensation," in *Proc. of Antennas and Propagation (EUCAP), 2012 6th European Conference on*, Page(s): 2789-2793, 2012. Article (CrossRef Link)
[19] Shi, Y, Ebethart, R. C., "Empirical study of Particle swami optimization," *Proceedings of the World Multiconference on Systemics, Cybemetics and Informaties*, Orlando, FL, 2000, 1945-1950. Article (CrossRef Link)
[20] Yi Xu, Guosen Yue, and Shiwen Mao, "User grouping for Massive MIMO in FDD systems: New design methods and analysis," *IEEE Access Journal, Special Section on 5G Wireless Technologies: Perspectives of the Next Generation Mobile Communications and Networking*, vol.2, no.1, pp.947-959, Sept. 2014. Article (CrossRef Link)

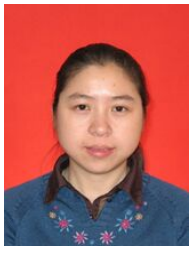

Guomei Zhang is currently an assistant professor in the School of Electronic and Information Engineering, Xi'an Jiaotong University, Xi'an, China. Her research interests include OFDM, MIMO, CoMP and Massive MIMO techniques in mobile communications systems.

Bing Wang is currently a graduate student in the School of Electronic and Information Engineering, Xi'an Jiaotong University, Xi'an, China. His research interests include massive MIMO and 3D MIMO techniques.

Guobing Li is currently an assistant professor in the School of Electronic and Info rmation Engineering, Xi'an Jiaotong University, Xi'an, China. His research interest s include wireless relay network, MIMO techniques and physical layer security.

Fei Xiang is a communication engineer in the Department of Baseband Algorithm, R&D center of ZTE Corporation, Xi'an, 710065, P. R. China.
His main research fields are in the algorithm design and application research or physical layer data-processing system of LTE and 5G.

Gangming Lv is currently an assistant professor in the School of Electronic and Information Engineering,Xi'an Jiaotong University, Xi'an, China. His research interests include mobile communications, massive MIMO and QoS guarantee in wireless communications systems.